ISLANDING DETECTION IN A MICROGRID ENVIRONMENT

A DISSERTATION

Submitted in partial fulfillment of the requirements for the award of the degree of

MASTER OF TECHNOLOGY

in

ELECTRICAL ENGINEERING

(With Specialization in Power System Engineering)

By

NIDHI GUPTA

DEPARTMENT OF ELECTRICAL ENGINEERING
INDIAN INSTITUTE OF TECHNOLOGY ROORKEE
ROORKEE - 247 667 (INDIA)

MAY 2015

CANDIDATE'S DECLARATION

I hereby declare that the work which is being presented in this seminar report entitled **"ISLANDING DETECTION IN A MICROGRID ENVIRONMENT"** in partial fulfillment of the requirement of the award of Degree of **Master of Technology** in **Electrical Engineering with specialization in Power System Engineering**, submitted to the Department of Electrical Engineering, Indian Institute of Technology, Roorkee, India is an authentic record of the work carried out during the period from June 2014 to May 2015 under the supervision of **Dr. Premalata Jena** and **Dr. Bhavesh R. Bhalja**, Department of Electrical Engineering, Indian Institute of Technology, Roorkee. The matter presented in this seminar has not been submitted by me for the award of any other degree of this institute or any other institute.

Date: 22/05/2015

Place: Roorkee

Nidhi Gupta

(Nidhi Gupta)

CERTIFICATE

This is to certify that the above statement made by the candidate is correct to best of my knowledge.

(Dr. Bhavesh R. Bhalja)
Assistant Professor
Department of Electrical Engineering,
Indian Institute of Technology,
Roorkee-247667, India

(Dr. Premalata Jena)
Assistant Professor
Department of Electrical Engineering,
Indian Institute of Technology,
Roorkee-247667, India

ACKNOWLEDGEMENT

I take this opportunity to express my sincere gratitude to my project guide **Dr. Premalata Jena**, Assistant Professor, Department of Electrical Engineering, Indian Institute of Technology, Roorkee and co-guide **Dr. Bhavesh R. Bhalja**, Assistant Professor, Department of Electrical Engineering, Indian Institute of Technology, Roorkee for their valuable guidance, support, encouragement and constructive criticism, during the course of my work, and in preparation of this seminar report, for which I will be indebted to them.

Nidhi Gupta

ABSTRACT

The island is an unregulated power system. Its behavior is unpredictable due to the power mismatch between the load and generation and lack of voltage and frequency control. For the micro grids to be operated safely and consistently, it is necessary to detect the islanding condition in a grid in a very quick and accurate manner.

This thesis report provides a concise view of the development of a power system network using Real Time Digital Simulator (RTDS) and then different passive islanding detection techniques are discussed. A new islanding detection method based on the cumulative sum of the superimposed power is also proposed in the thesis which works satisfactorily in different islanding and non-islanding conditions.

TABLE OF CONTENTS

LIST OF FIGURES

LIST OF TABLES

1 INTRODUCTION

1.1 Distributed Generation (DG)

In an electric grid, the electrical energy is transferred from the generating stations to consumers. Due to the ongoing increasing demand of the electrical energy, there is a necessity to build new transmission and distribution lines. But to build new T&D lines or to upgrade them is a very complex task. So to avoid the complexity, the distributed generations are becoming more popular nowadays due to the various advantages offered by them.

The use of small-scale power generating technologies (typically in the range of 1 kW-10,000 kW) is called the distributed generations which are located near to the load where the demand of electrical energy arises. These are also known as distributed resources (DR), on-site power generation, dispersed power (DP) or distributed energy resources (DER). DGs have become a significant alternative to up gradation of power system structure due to the inventions in power electronic equipments like high voltage Insulated Gate Bipolar Transistors (IGBT) and developments in the new renewable power generating technologies like solar, wind etc.

Types of distributed generators include induction generator, synchronous generators and asynchronous generators. Wind power generations are the example of induction generators. Synchronous machines are most commonly used with internal combustion machines, gas turbines, and small hydro dams. And the asynchronous generators are commonly used with micro turbines, photovoltaic and fuel cells.

1.1.1 Benefits of Distributed Generations

The various advantages offered by the distributed generations are:

- Distribution generations can be placed in any location in the distributed system. Hence where the need arises, DGs can be installed and it gives great flexibility to supply the demand of electrical energy.
- DGs reduce transmission and distribution losses.
- Improve voltage profile and power quality of the power system.
- Reduce loading on the substation during peak hours.

- DGs reduce the requirement of building new T&D lines.
- The transmission and distribution system disturbances are minimized by the DG as these are installed at the locations nearer to the load. Thus they can improve the grid reliability.
- Due to occurrence of natural disasters or any interruptions, electricity is interrupted. So DGs provide additional generation and improves security of the system.

1.1.2 Technical Challenges Facing Distributed Generations

Although various advantages being offered by the DGs but as far as protection system is concerned, DGs have to face different technical challenges. There are various integration challenges which include:

- When DGs are integrated into the distribution system at low voltage levels, it can cause reverse power flow but initially distribution feeders are designed for unidirectional power flow. Hence bidirectional power flows in case of DG and it leads to coordination problem, voltage control and fault current distribution complications.
- From the interaction of DG unit control system, local oscillations can occur requiring a complete small-disturbance i.e. steady state stability analysis.
- Increased short circuit levels
- Coordination of Multiple generators
- Islanding i.e. loss of mains problem.

1.2 Micro Grid

When it was not possible to interconnect with the host power system in remote areas, some small autonomic electric grids had been created in the past [1]. These small electric grids when combined are called a microgrid. Initially, fossil-fuel power generation technology has been the common option to supply the electrical energy in these micro grids due to the advantages of their flexibility and low investment costs. However, integration of green generation technologies i.e. wind, solar, and hydro power has been very important in these grids as these technologies provide feasibility of economical and technical operation.

In paper [1] author described microgrid as a combination of different units of Distributed Generation (DG), loads and Energy Storage Systems (ESS) which works in synchronization

to supply electrical energy and they are connected at distribution voltage level to main grid at one connection point, which is called Point of Common Coupling (PCC). An example of microgrid is shown in the Fig.1.

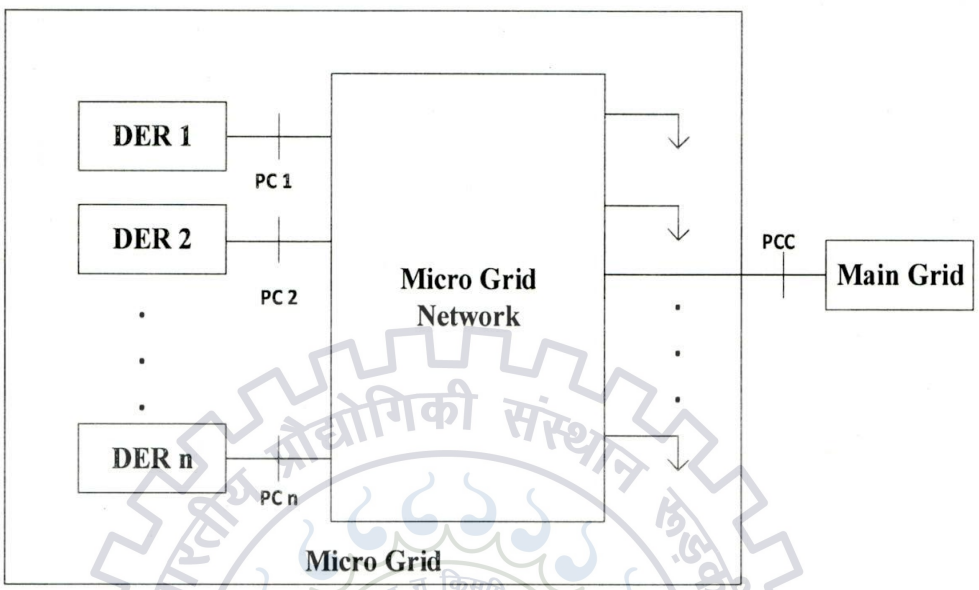

Fig. 1. Schematic diagram of a generic multiple-DER microgrid

1.3 Islanding

Nowadays distributed generations (DGs) are being integrated into the distribution system due to the increased demand of the electrical energy. Although, to protect the modern distribution network, conventional protection system has been modernized and upgraded, but still there are some issues needed to be considered. One such issue is islanding.

Islanding is very important protection issue when concerned with the DGs. Islanding is an unregulated power system. Islanding of a grid connected DG is a phenomenon when the local networks containing such DGs gets disconnected but the local loads are been supplied by the DGs without the control of utility [2]. As shown in the Fig.2, generally, a distribution system does not contain any source of active power generation and if a fault occurs in the upstream of transmission line, this doesn't obtain any active power. But in case of a DG this assumption is not valid. In current practice, it is required that DG should be disconnected instantly from the main grid if islanding occurs.

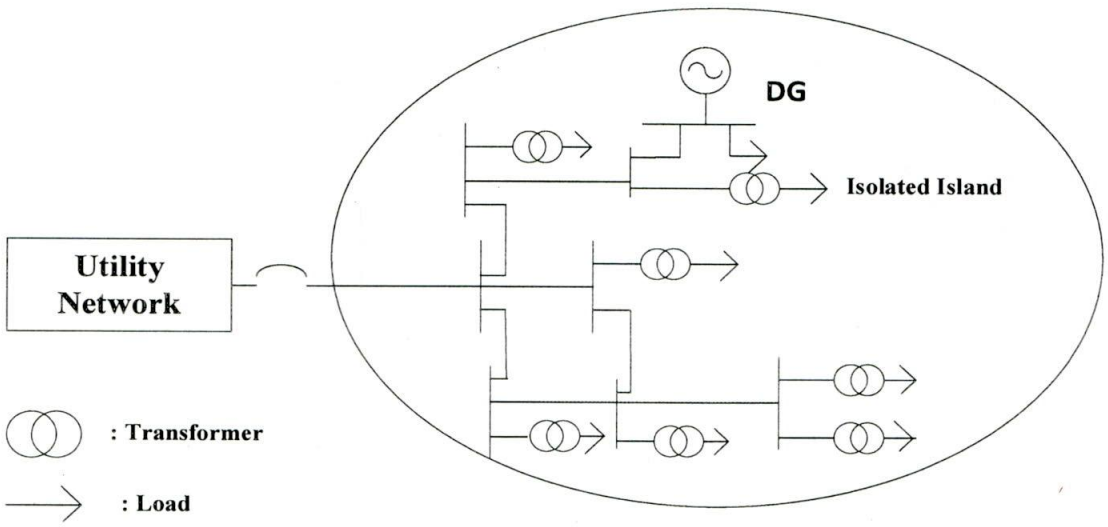

Fig.2 Scenario of Islanding Operation

An electric grid connected with DGs can be operated in two modes i.e. the grid-connected and isolated modes, and it also handles the transitions of these modes. In the grid-connected mode, both the main power system and microgrid can supply load demand of electrical energy. In the isolated or islanded mode, the total power generation by the microgrid and the total load demand should be balanced. Islanding can be scheduled (intentional) or unscheduled (unintentional). Scheduled islanding can take place due to scheduled maintenance or to avoid degradation of power quality. Unscheduled islanding can happen due to different faults and some events which are not known to the system. If islanding is not detected in a certain time, it can lead to many negative impacts on the generators and connected loads. According to IEEE Std. 1547-2003, fast and accurately detection of islanding condition is very important for reliable operation of the distribution system with the DG [3] and also proper islanding detection is essential for personnel safety and proper function of microgrid.

1.4 Issues related with Islanding

Although islanding operation offers some advantages, yet there are disadvantages as well which includes [2]:

- When islanding occurs into the system, it can threaten the safety of line workers after opening of main sources.
- With the system disconnection, the voltage and frequency fluctuations occur and they may not be sustained to their standard values.

- DG's out of phase reclosing is the result of instantaneous reclosing. And due to this large mechanical torques are formed that can be harmful to generators or prime movers. This can also create transients and damage the utility and consumer equipments.
- Loss of main grid also results various risks which include degradation of other electric modules as a result of changes in voltage & frequency.

Due to the above reasons, if islanding is not being detected instantly it can result great damage to the whole system. Hence it is extremely important to identify the islanding condition fast and accurately.

1.5 Objective

Islanding is a very important protection issue with distributed generation. The objective of this thesis to review the conventional passive islanding detection techniques and to develop a new islanding detection method which works efficiently in power distribution network when multiple DGs are being integrated. This thesis work examines a new islanding detection method based on the cumulative sum of the superimposed power and it is compared with the conventional methods i.e. Rate of change of power (ROCOP) and Rate of change of frequency (ROCOF) for various islanding and non-islanding conditions.

1.6 Organization of the Thesis

Chapter 1 begins with the distributed generation, its benefits and protection challenges. It also explains the microgrid, islanding operation and issues related with islanding.

Chapter 2 gives the literature review and describes the conventional passive islanding detection methods, their advantages and disadvantages.

Chapter 3 illustrates the simulation model of the system under study. And the required and necessary data are also given in this chapter. Also describes the proposed method for islanding detection and different islanding and non islanding conditions are mentioned.

In Chapter 4 all the results and discussions are given for various islanding and non-islanding conditions and a comparison of proposed method with the existing techniques is also given.

Chapter 5 summarizes the thesis work and conclusion is given in the end.

2 LITERATURE REVIEW

2.1 Review of Islanding Detection Methods

In general, the islanding condition is detected by monitoring the output parameters of DG and system parameters and then from changes in these parameters it is decided whether the islanding condition has occurred or not. In [2], various techniques are described to detect the islanding condition like, remote and local techniques. Local methods are further classified into passive methods, active methods and hybrid of passive and active as shown in Fig. 3. This report focuses on the passive islanding techniques based on certain parameters such as nuisance tripping of DG due to different non-islanding events, non detection zone (NDZ), ability to handle various Distributed Generators etc.

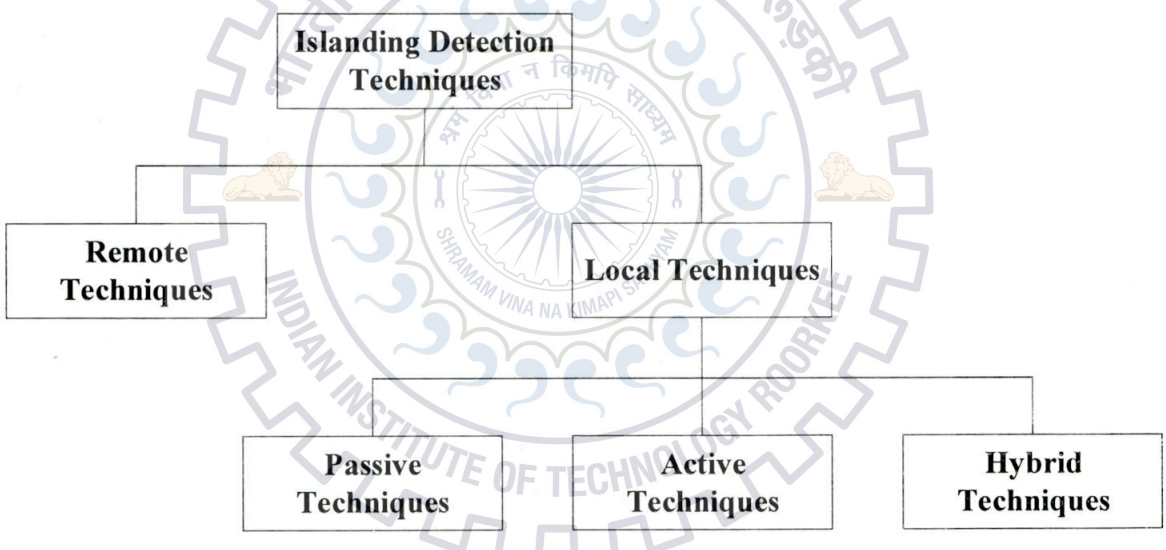

Fig.3 Islanding Detection Techniques

2.2 Conventional Passive Islanding Detection Methods

Passive methods are based on measuring the parameters of system such as voltage, frequency, active power and reactive power etc. at the DG output when islanding occurs. These parameters changes to a great extent at the time of islanding. There is a threshold point required for these parameters to differentiate between the islanding and non-islanding conditions. In order to discriminate islanding situation from other condition of disturbances,

there should be special care for selecting the threshold point. Passive detection methods are low-cost and easy to implement. These methods are very fast and also don't introduce the disturbance into the system. One of the disadvantages of these methods is the large non detectable zone (NDZ). NDZ is the area where they are not able to detect islanding.

There are a variety of passive detection methods which are as below:

2.2.1. Rate of change of output power

In [4], it is described that once islanding occurs, rate of change of output power (ROCOP) at the DG side i.e. *dP/dt,* will be higher than ROCOP before the islanding of DG under the same load change.

In [5], different tests based on this method have been done which results that this technique is more efficient with DG's unbalanced load of distribution system compare to balanced load.

2.2.2. Rate of change of frequency

In [6], islanding detection method based on the rate of change of frequency (ROCOF) is described which demonstrates that it is a passive method based on the mismatch between DG active power and loads at the instant of islanding. The rate of change of frequency is calculated from the swing equation of generator given by,

$$\frac{\Delta f}{\Delta t} = \Delta P . \frac{f}{2HG} \qquad (2a)$$

Where, ΔP is the active power mismatch between DG and loads at the DG location,

f is the system frequency,

H is the inertia constant of the system/generator,

G is the rated capacity of the system/ generator.

When islanding occurs, the value of the ROCOF i.e. *df/dt*, will be very high. Paper [6] explains that ROCOF relay will trip if measured value of ROCOF is greater than the threshold point for a certain time period. The threshold is selected so that relay operates only for islanding situation not for different non-islanding conditions i.e. load change.

One of the disadvantages of this method is that it works efficiently for large active and reactive power mismatch and doesn't operate when generating power capacity of DG equals

the local loads in the formed island. Hence it is preferred to use rate of change of frequency together with ROCOP for lower power mismatches.

2.2.3 Rate of change of frequency over power

From equation (2a), it can be referred that rate of change of frequency over power i.e. *df/dP* in a smaller system is higher than the large capacity power system. In paper [7], this concept is used to determine islanding condition. In this paper it has been proved by the test results that if power mismatch between DG and local loads is small then this method is more effective to detect islanding situation than ROCOF over time.

2.2.4 Voltage unbalance

At the time of islanding for larger load change, it is easy to detect the islanding condition by measuring the parameters like voltage amplitude, frequency and phase change. But these methods will not work for small load change. Due to the single phase loads in the distribution networks, DG load balance will be changed by the islanding. Also, unbalance in voltage will take place even for small load change since network condition changes [8]-[9].

2.2.5 Harmonic Detection

For DGs which are inverter based, if the load configuration changes, it results the change in harmonic currents [8]. In [8] it is described that to detect the islanding condition, voltage harmonics are being utilized. One technique is to measure change in the terminal voltage total harmonic distortion at DG side before islanding and after islanding condition. It is also good to monitor the change in DG's voltage third harmonics at the instant of islanding [10]-[11].

2.2.6 Change in the reactive power

Other passive islanding detection method uses parameters like, voltage, active power and frequency directly or indirectly. The method of active power mismatch utilizes the imbalance between DG's generation active power and consumption of the loads active power but this method uses the reactive power imbalance.

Paper [12] describes that the detection criteria used in this method is the rate of change of voltage of DG over consumption of loads reactive power i.e. $\partial V_{DG}/\partial Q_{load}$. Hence it is a voltage based islanding detection technique.

It has been found by the simulation results for islanding and non-islanding conditions that this approach is very effective even if reactive power imbalance is one percent whereas the ROCOF and ROCOV methods fail in this condition. Also, this method has small NDZ compare to ROCOV method.

2.2.6 Change in the impedance

The impedance of the main system is smaller than impedance of islanded system. This concept is utilized to detect the islanding condition in the paper [13]. When a section of the system gets disconnected from main grid, its impedance will increase. By monitoring the system impedance, islanding situation can be detected.

3 PROPOSED TECHNIQUE AND SYSTEM STUDIED

3.1 System Studied

Fig. 4 shows the single line diagram of a power distribution network. This power system and the following data of the various parts of the network are taken from the paper [14].

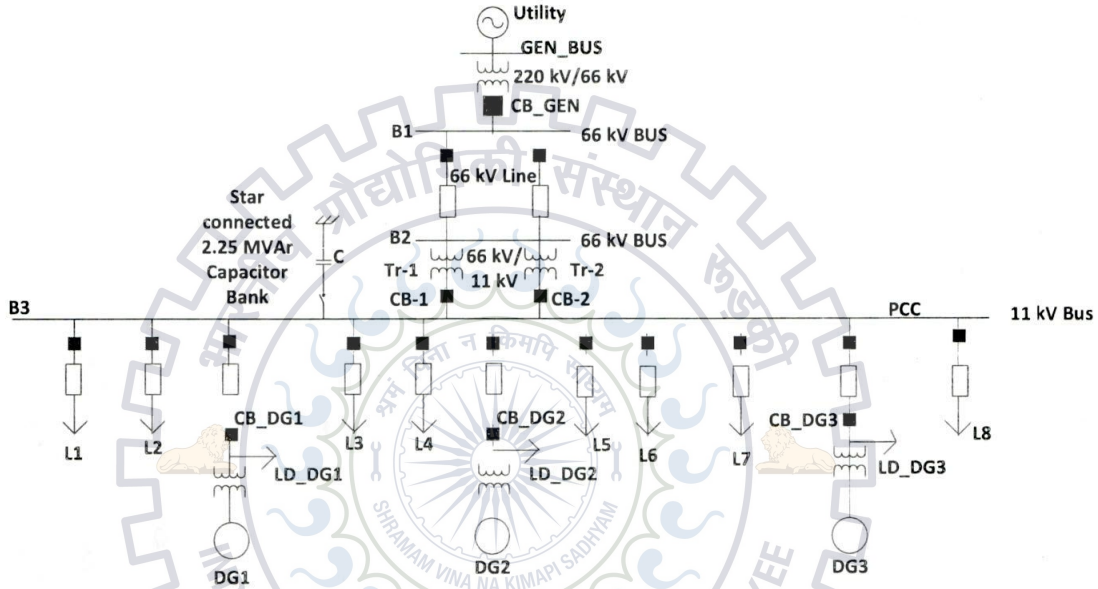

Fig. 4. Single line diagram of a power system network

In this network, a transmission system of 220 kV, 50 Hz is modeled using voltage source and impedance. A 66 kV substation, which is emanated from 220 kV substation, connects two 66 kV sub-transmission lines between buses B1 and B2. In this system, there are two transformers (Tr-1 and Tr-2) of 11 MVA each which are used to convert 66 kV into 11 kV. Eleven distribution feeders are connected from the bus B3 at 11 kV. In this distribution network, there are three Distributed generators each of 9 MVA capacity and connected to 11 kV systems with the help of a 0.415-kV/11-kV, 9-MVA transformer. The details of line parameters, distribution feeder parameters, and generator and exciter parameters are given in the Table I, II and III [16].

TABLE I. LINE PARAMETERS

Type of conductor	Voltage (kV)	Area of cross-section(mm^2)	Resistance (Ω/km)	Inductance (Ω/km)
Rabbit	11	61.9	0.5449	0.305
Dog	66	118.45	0.2745	0.283

TABLE II. DISTRIBUTION FEEDER PARAMETERS

Load	Length (km)	P (kW)	Q (kVAR)
L_1	2.70	1693	556
L_2	3.10	1919	630
L_3	5.20	1480	486
L_4	2.50	1791	588
L_5	3.70	794	260
L_6	11.11	1772	582
L_7	2.90	1490	489
L_8	4.50	1970	647
LD-1	3.10	570	187
LD-2	6.20	570	187
LD-3	5.30	570	187

TABLE III. SYNCHRONOUS GENERATOR AND EXCITER PARAMETERS

Synchronous generator parameters:	
Rated RMS line to neutral voltage (Vrms)	0.239 kV
Rated RMS line current (Irms)	12.52 kA
Base angular frequency (w)	314.15 (rad)
Inertia constant (H)	3.117 (sec)
Mechanical friction and windage (Dm)	0.04 (pu)
Neutral series resistance (Rs)	1.0E5 (pu)
Neutral series reactance (Xs)	0 (pu)
Iron loss resistance (Rm)	0.5 (pu)
Exciter Parameters:	
Rectifier smoothing time constant (T1)	0.02 (sec)
Controller lead time constant (TA)	1.5 (sec)
Controller lag time constant (TB)	1.0 (sec)
Exciter time constant (TE)	0.02 (sec)
Exciter gain (K)	100 (pu)
Maximum field voltage (EMAX)	5 (pu)
Minimum field voltage (EMIN)	5 (pu)
L-G Voltage base (RMS)	0.239 (KV)
Line current base (RMS)	12.52 (KA)

3.2 Simulation Model

The power system shown in Fig. 4 is simulated in RSCAD software. The simulated power system network is shown in Fig. 5. At the DG-1 location, voltage and current signals are acquired using Real time digital simulator (RTDS). RSCAD software is used to generate the test data and the performance of the different method is evaluated in MATLAB software. The Bergeron line model is used to represent the transmission and distribution lines in the system.

The various islanding and non-islanding situations that can be simulated are as follows [16]:

(a) Islanding conditions:

- Islanding of DG due to opening of the circuit breaker at main substation i.e. CB_GEN.

- Islanding due to opening of the circuit breakers CB1 and CB2.

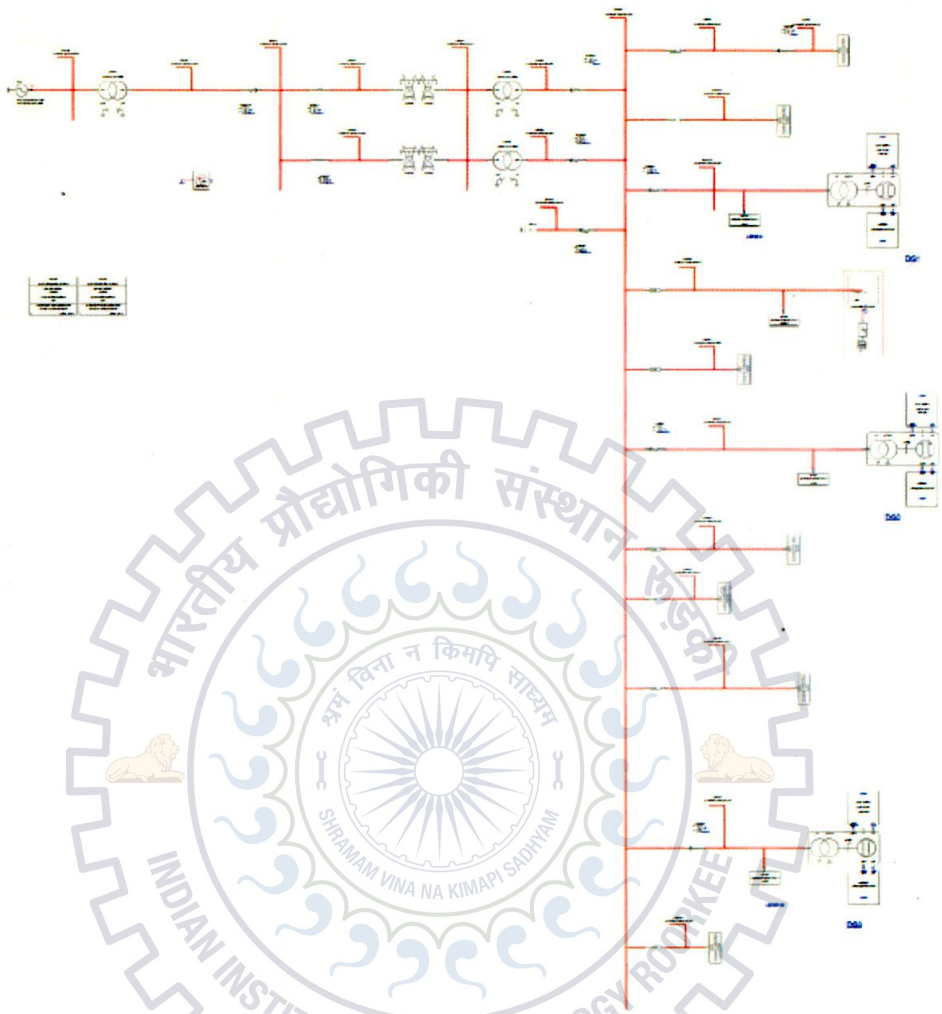

Fig.5. Simulated system in RSCAD Software

(b) Non-islanding conditions:

- unexpected change in the load located at target DG-1,
- switching ON or OFF of load on 11-kV bus,
- switching ON or OFF of capacitor (C) located on 11 kV bus,
- switching ON or OFF of one of the 66-kV transmission line,
- switching ON or OFF of transformer Tr-1 or Tr-2,
- tripping off other DGs i.e. DG- 2 or DG-3.

3.3 Proposed Islanding Detection Method

In thesis a new method of islanding detection is proposed which is cumulative sum of the superimposed power. In this method, firstly the voltage and current signals are acquired at the DG-1 location using RSCAD software. Then three phase instantaneous power output at the DG-1 location is calculated using these voltages and current signals as given by:

$$P_{DG} = V_a.I_a + V_b.I_b + V_c.I_c \qquad (3a)$$

Where, V_a, V_b , V_c and I_a, I_b, I_c are the instantaneous voltage and current signals respectively at the DG-1 location. Single phase instantaneous power at DG location has been derived below for normal, islanding and non-islanding condition:

(a) For normal condition:

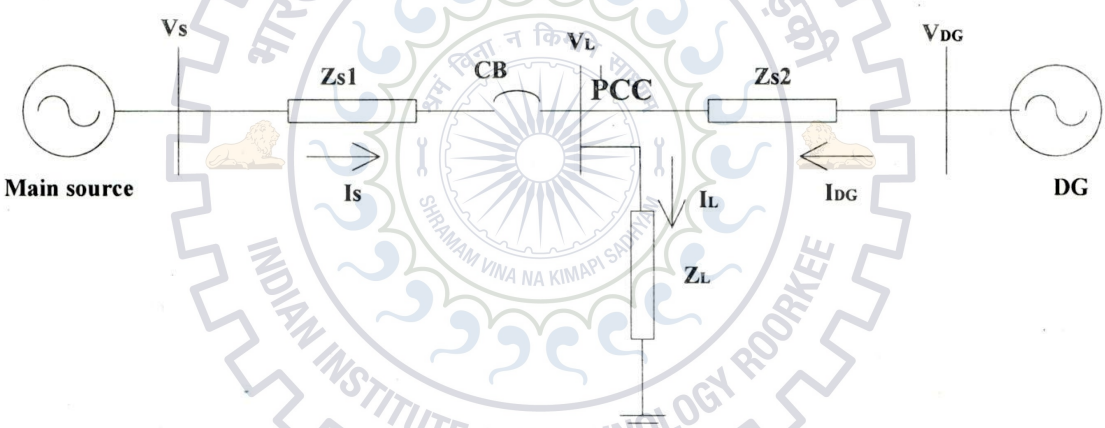

Fig.6. Schematic diagram of a system with DG during normal condition

From Fig.6, $I_s + I_{DG} = I_L$

$$V_{DG} = |V_{DG}|.Sin\ \omega t$$

$$V_s = |V_s|.Sin\ (\omega t + \varnothing)$$

$$V_L = |V_L|.Sin(\omega t + \alpha)$$

$$I_L = |V_L|.\frac{Sin\ (\omega t + \alpha)}{Z_L}$$

$$I_s = \frac{V_s - V_L}{Z_{s1}}$$

$$I_s = \frac{|V_s|.Sin\,(\omega t + \varnothing)}{Z_{s1}} - \frac{|V_L|.Sin\,(\omega t + \alpha)}{Z_{s1}}$$

Therefore, $I_{DG} = I_L - I_s$

$$I_{DG} = \left(|V_L|.Sin\,(\omega t + \alpha)\right).\left[\frac{1}{Z_L} + \frac{1}{Z_{s1}}\right] - \frac{|V_s|.Sin\,(\omega t + \varnothing)}{Z_{s1}} \quad (3b)$$

$$V_{DG} = Z_{s2}.I_{DG} + V_L$$

$$V_{DG} = |V_L|.Sin\,(\omega t + \alpha) + |V_L|.Sin\,(\omega t + \alpha).Z_{s2}.\left[\frac{1}{Z_L} + \frac{1}{Z_{s1}}\right] - \left(\frac{Z_{s2}}{Z_{s1}}\right).|V_s|.Sin\,(\omega t + \varnothing)$$

$$V_{DG} = |V_L|.Sin\,(\omega t + \alpha)\left[1 + Z_{s2}.\left\{\frac{1}{Z_L} + \frac{1}{Z_{s1}}\right\}\right] - \left(\frac{Z_{s2}}{Z_{s1}}\right).|V_s|.Sin\,(\omega t + \varnothing) \quad (3c)$$

Instantaneous per phase power output at DG,

$$P_{DG} = V_{DG}.I_{DG} \quad (3d)$$

Substituting equation (3b) and (3c) in (3d), P_{DG} can be derived for normal condition.

(b) For islanding condition:

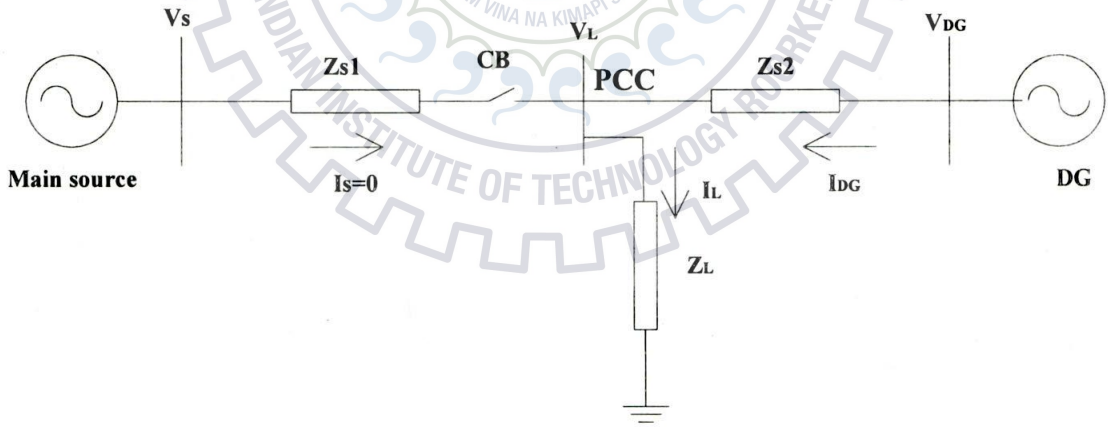

Fig.7. Schematic diagram of a system with DG during islanding condition

From Fig.7 after islanding of the system, CB opens and $I_s = 0$;

$$I_{DG} = I_L$$

$$I_{DG} = \frac{V_{DG} - |V_L|}{Z_{s2}}$$

$$I_L = \frac{V_L}{Z_L}$$

$$I_L = \frac{|V_L|.Sin\,(\omega t + \alpha)}{Z_L} = I_{DG}$$

$$V_{DG} = Z_{s2}\,.I_{DG} + V_L$$

$$V_{DG} = \left(\frac{Z_{s2}}{Z_L}\right).|V_L|.Sin\,(\omega t + \alpha) + |V_L|.Sin\,(\omega t + \alpha)$$

$$V_{DG} = |V_L|.Sin\,(\omega t + \alpha).\left[1 + \frac{Z_{s2}}{Z_L}\right]$$

Instataneous per phase power output at DG in islanding condition,

$$P_{DG} = V_{DG}.I_{DG}$$

$$= |V_L|.Sin\,(\omega t + \alpha).\left[1 + \frac{Z_{s2}}{Z_L}\right] + \frac{|V_L|.Sin\,(\omega t + \alpha)}{Z_L}$$

$$P_{DG} = \left\{\frac{|V_L|.Sin\,(\omega t + \alpha)}{Z_L}\right\}^2.(Z_L + Z_{s2}) \qquad (3e)$$

Above equation (3e) gives single phase instantaneous power for islanding condition.

(c) For Non-islanding condition i.e. capacitor switching at PCC:

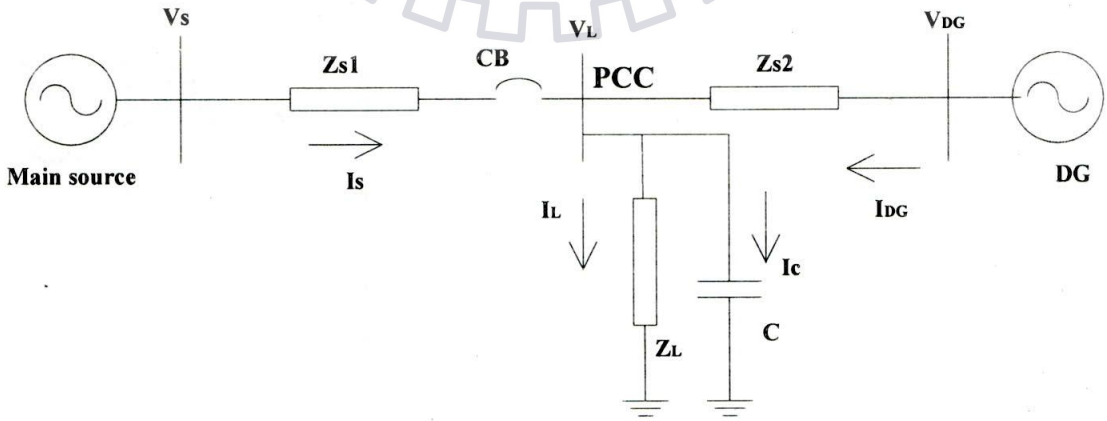

Fig.8. Schematic diagram of a system with DG during non-islanding condition

From Fig. 8 after switching on the capacitor at PCC,

$$I_s + I_{DG} = I_L + I_C;$$

$$I_s = \frac{V_s - V_L}{Z_{s1}}$$

$$I_s = \frac{|V_s|.Sin\,(\omega t + \varnothing) - |V_L|.Sin\,(\omega t + \alpha)}{Z_{s1}}$$

$$I_L = \frac{|V_L|.Sin\,(\omega t + \alpha)}{Z_L}$$

$$I_C = C.\frac{dV_L}{dt}$$

$$= C.\omega.|V_L|.Cos\,(\omega t + \alpha)$$

Therefore, $I_{DG} = I_L + I_C - I_s$

$$I_{DG} = \frac{|V_L|.Sin\,(\omega t + \alpha)}{Z_L} + C.\omega|V_L|.Cos\,(\omega t + \alpha) + \frac{|V_L|.Sin\,(\omega t + \alpha)}{Z_{s1}} - \frac{|V_s|.Sin\,(\omega t + \varnothing)}{Z_{s1}}$$

$$I_{DG} = V_L.Sin\,(\omega t + \alpha)\left[\frac{1}{Z_L} + \frac{1}{Z_{s1}}\right] + C\omega.|V_L|.Cos\,(\omega t + \alpha) - \frac{|V_s|.Sin\,(\omega t + \varnothing)}{Z_{s1}} \quad (3f)$$

$$V_{DG} = Z_{s2}.I_{DG} + V_L \quad (3g)$$

Instantaneous per phase power output at DG in non-islanding condition,

$$P_{DG} = V_{DG}.I_{DG}$$

Substituting equation (3f) and (3g) in above eq., P_{DG} can be derived for non-islanding condition.

For the determination of three phase instantaneous power equation, it is assumed that 3-φ system is a balanced system. It means the phase difference between voltage and current of one phase to their adjacent phase is 120° and each phase amplitude of voltage and current is same.

The three phase voltages and currents are:

$$V_a = V_m\,Sin\,\omega t$$

$$V_b = V_m\,Sin\,(\omega t - 120)$$

$$V_c = V_m\,Sin\,(\omega t + 120)$$

$$I_a = I_m \, Sin\,(\omega t - \varnothing)$$

$$I_b = I_m \, Sin\,(\omega t - \varnothing - 120)$$

$$I_c = I_m \, Sin\,(\omega t - \varnothing + 120)$$

Where ⌀=phase difference between voltage and current of each phase.

Now, the instantaneous power of each phases are:

$$V_a . I_a = V_m . I_m \; Sin\,\omega t . Sin\,(\omega t - \varnothing) \qquad (3h)$$

$$V_b . I_b = V_m . I_m \; Sin\,(\omega t - 120) . Sin\,(\omega t - \varnothing - 120) \qquad (3i)$$

$$V_c . I_c = V_m . I_m \; Sin\,(\omega t + 120) . Sin\,(\omega t - \varnothing + 120) \qquad (3j)$$

The total instantaneous three phase power is given by the equation (2), hence substituting eq. (3h), (3i) and (3j) in eq. (2a):

$$P = V_m . I_m \, Sin\,\omega t . Sin\,(\omega t - \varnothing) + V_m . I_m \, Sin\,(\omega t - 120) . Sin\,(\omega t - \varnothing - 120) + V_m . I_m \, Sin\,(\omega t + 120) . Sin\,(\omega t - \varnothing + 120)$$

$$P = V_m . I_m \, [Sin\,\omega t . Sin\,(\omega t - \varnothing) + Sin\,(\omega t - 120) . Sin\,(\omega t - \varnothing - 120) + Sin\,(\omega t + 120) . Sin\,(\omega t - \varnothing + 120)]$$

$$P = \left(\frac{1}{2}\right) . V_m . I_m \, [2 . Sin\,\omega t . Sin\,(\omega t - \varnothing) + 2 . Sin\,(\omega t - 120) . Sin\,(\omega t - \varnothing - 120) + 2 . Sin\,(\omega t + 120) . Sin\,(\omega t - \varnothing + 120)]$$

$$P = \left(\frac{1}{2}\right) . V_m . I_m \, [Cos\,\varnothing - Cos\,(2\omega t - \varnothing) + Cos\,\varnothing - Cos\,(2\omega t - 240 - \varnothing) + Cos\,\varnothing - Cos\,(2\omega t + 240 - \varnothing)]$$

$$P = \left(\frac{1}{2}\right) . V_m . I_m \, [3\,Cos\,\varnothing - Cos\,(2\omega t - \varnothing) - Cos\,(2\omega t - 240 - \varnothing) - Cos\,(2\omega t + 240 - \varnothing)]$$

$$P = \left(\frac{1}{2}\right) . V_m . I_m \, [3\,Cos\,\varnothing - Cos\,(2\omega t - \varnothing) - 2\,Cos\,(2\omega t - \varnothing) . Cos\,(240)]$$

$$P = \left(\frac{1}{2}\right) . V_m . I_m \, [3\,Cos\,\varnothing - Cos\,(2\omega t - \varnothing) - 2\,Cos\,(2\omega t - \varnothing) . (-1/2)]$$

$$P = \left(\frac{1}{2}\right) . V_m . I_m \, [3\,Cos\,\varnothing - Cos\,(2\omega t - \varnothing) + Cos\,(2\omega t - \varnothing)]$$

$$P = \left(\frac{1}{2}\right) . V_m . I_m . 3 . Cos\,\varnothing$$

$$P = 3 . \left(\frac{V_m}{\sqrt{2}}\right) . \left(\frac{I_m}{\sqrt{2}}\right) . Cos\,\varnothing$$

$$P = 3 . V_{rms} . I_{rms} . Cos\,\varnothing$$

The above equation is a three phase power equation. Hence three phase power equation is a time independent equation.

Now superimposed power is given by the following equation:

$$P_s = P_i - P_{pre} \tag{3k}$$

Where, P_s is the superimposed power,

P_i is three phase islanding power at DG-1 location,

P_{pre} is the three phase power before islanding at DG-1 location.

After calculating superimposed power, the cumulative summation is calculated. The cumulative summation (cumsum) is the sequence of all partial sums of a sequence. Hence using the sampling frequency i.e. 1 kHz, all the samples of the superimposed power for one period is cumulatively summed up to given a sequence of samples. This cumsum is plotted in the MATLAB. Before islanding this cumsum will be zero because there is no islanding condition and islanding power *Pi* will be equal to the *Ppre*. For different islanding and non islanding conditions, this cumsum is plotted and compared with the conventional techniques ROCOP and ROCOF.

4 RESULTS AND DISCUSSION

The test system is simulated with a sampling frequency 1 KHz and the system frequency is 50Hz. So the no. of sample in a period is 20. Different islanding and non-islanding conditions are simulated on the test system in the RSCAD and the performance of proposed method is evaluated at DG-1 in the MATLAB and compared with the conventional passive methods i.e. ROCOP and ROCOF. Islanding condition is simulated by opening the main circuit breakers CB1 and CB2 at point of common coupling (PCC).

4.1 Results for Conventional techniques (ROCOP and ROCOF)

Different islanding and non-islanding conditions have been simulated for conventional schemes i.e. ROCOP and ROCOF and results are shown below in the figures. Fig.9 shows that simulation results given by the rate of change of power scheme during islanding condition (simulated by the tripping of circuit breakers CB1 and CB2) at different active power mismatch percentages i.e. 0%, 5%, 10% and 30%. A non islanding condition is also simulated in the figure by tripping off DG-3. In Fig.10 simulation results are given for ROCOP during islanding condition at 40%, 50%, 60% and 80% active power mismatch and non-islanding condition (switching off Tr-1). For ROCOP threshold has been taken 0.16 pu. Threshold has been decided by simulating all non-islanding conditions and setting to threshold to the greater than the maximum of all these values. Hence ROCOP relay will trip when the measured value of rate of change of power will be higher than threshold value for a certain period of time.

Similarly for ROCOF scheme various non-islanding and islanding conditions have been simulated and results are given. Fig.11 shows that simulation results given by the rate of change of frequency scheme during islanding condition (simulated by the tripping of circuit breakers CB1 and CB2) at different active power mismatch percentages i.e. 0%, 5%, 10% and 30%. A non islanding condition is also simulated in the figure by switching off one 66 kV Tx-line. In Fig.12 simulation results are given for ROCOF during islanding condition at 40%, 50%, 60% and 80% active power mismatch and non-islanding condition (switching on capacitor at PCC). For ROCOF threshold has been taken 0.6 Hz/sec. Threshold has been decided by simulating all non-islanding conditions and setting to threshold to the greater than

the maximum of all these values. Hence ROCOF relay will trip when the measured value of rate of change of power will be higher than threshold value for a certain period of time.

It is clear by the figures that ROCOP and ROCOF will operate only if active power mismatch is above 40%.

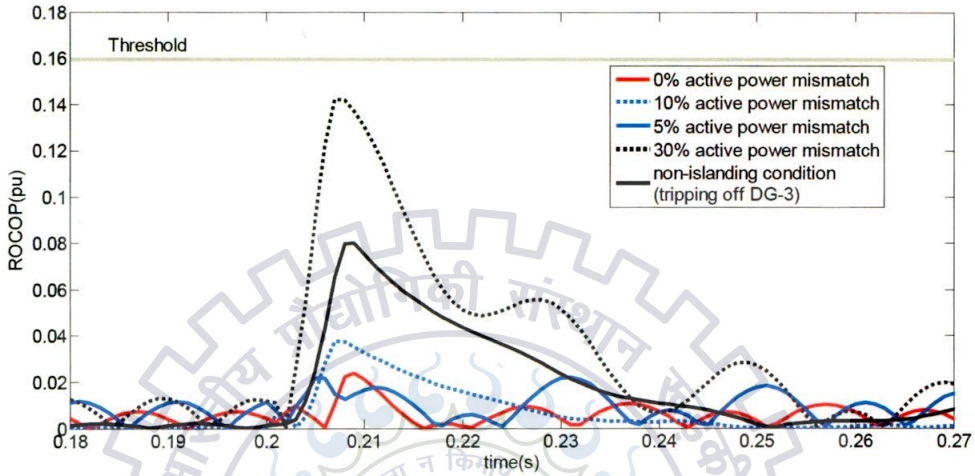

Fig.9. Rate of change of Power during islanding at different percentages of active power mismatch and a non-islanding condition (tripping off DG-3)

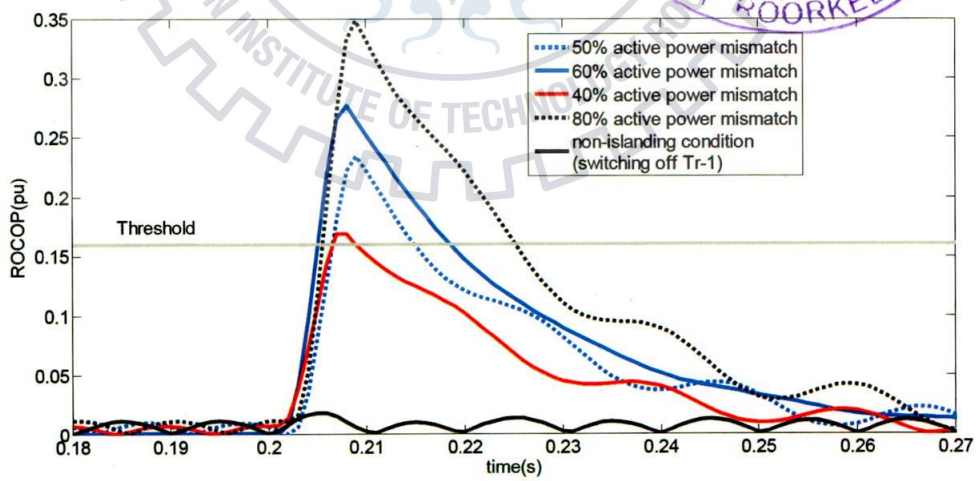

Fig.10. Rate of change of Power during islanding at different percentages of active power mismatch and a non-islanding condition (Switching off one Tr-1)

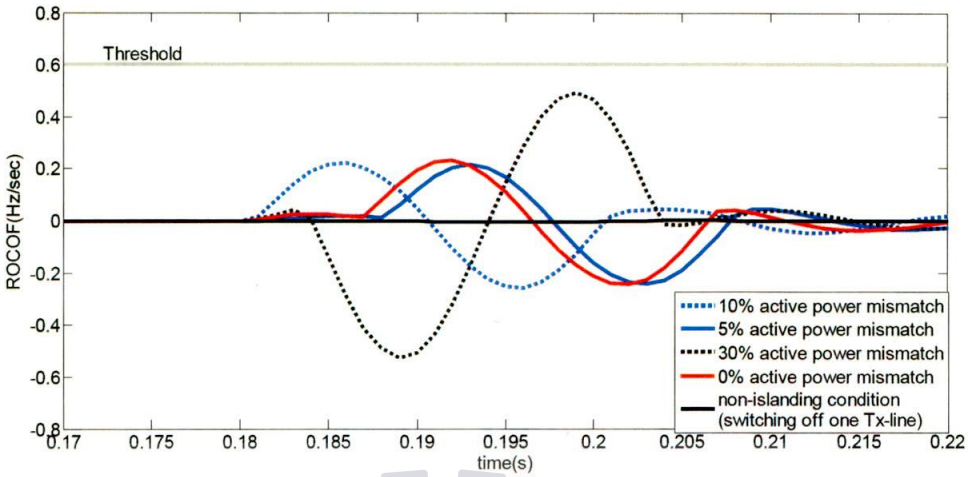

Fig.11. Rate of change of Frequency during islanding at different percentages of active power mismatch and a non-islanding condition (Switching off one Tx-line)

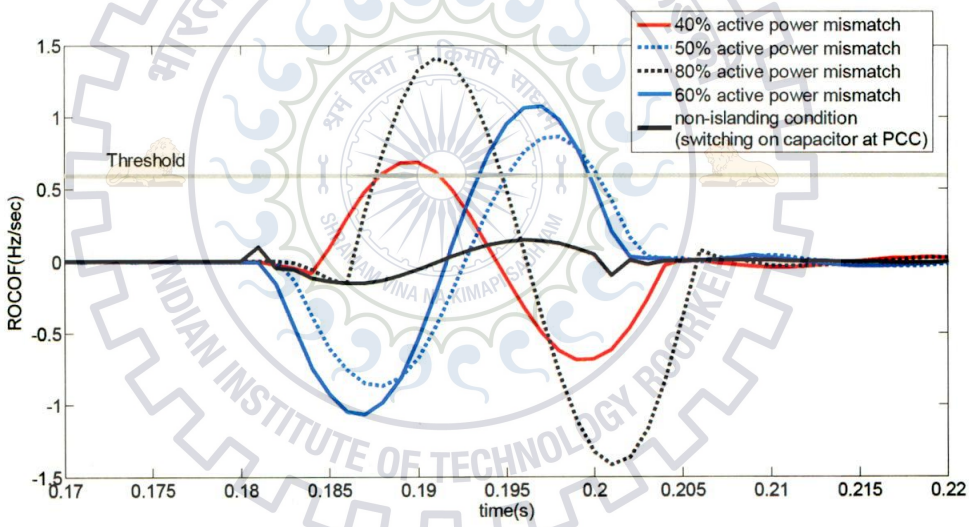

Fig.12. Rate of change of Frequency during islanding at different percentages of active power mismatch and a non-islanding condition (Switching on capacitor at PCC)

4.2 Results for Cumulative Sum of Superimposed Power

For proposed method, the first term to be calculated is total three phase instantaneous power at DG location. Fig.13, 14 and 15 shows the single phase instantaneous voltage, current and power at DG-1 location during islanding condition for phases 'a', 'b', and 'c'. In Fig. 16 total three phase instantaneous power is plotted at DG-1 during islanding condition. This figure shows that the magnitude of three phase instantaneous power decreases after the instant of

islanding. Fig.17 shows the superimposed power at DG-1 location during islanding at different active power mismatch i.e. 20%, 50% and 80% and a non-islanding condition (switching on capacitor at PCC). Before islanding the superimposed power is zero and after that its magnitude increases. This increase in the magnitude for islanding condition is greater than that for the non-islanding condition.

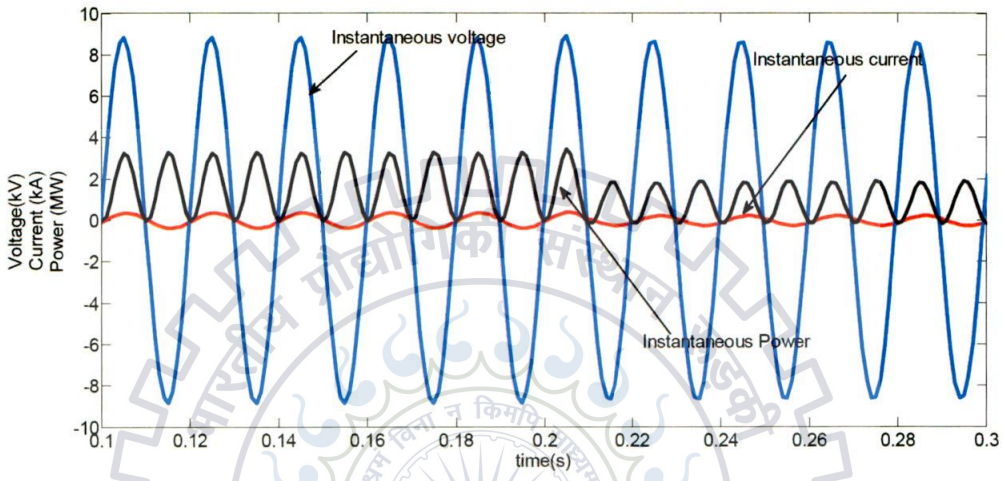

Fig.13. Single phase instantaneous voltage, current and power at DG-1 location during islanding condition for phase 'a'

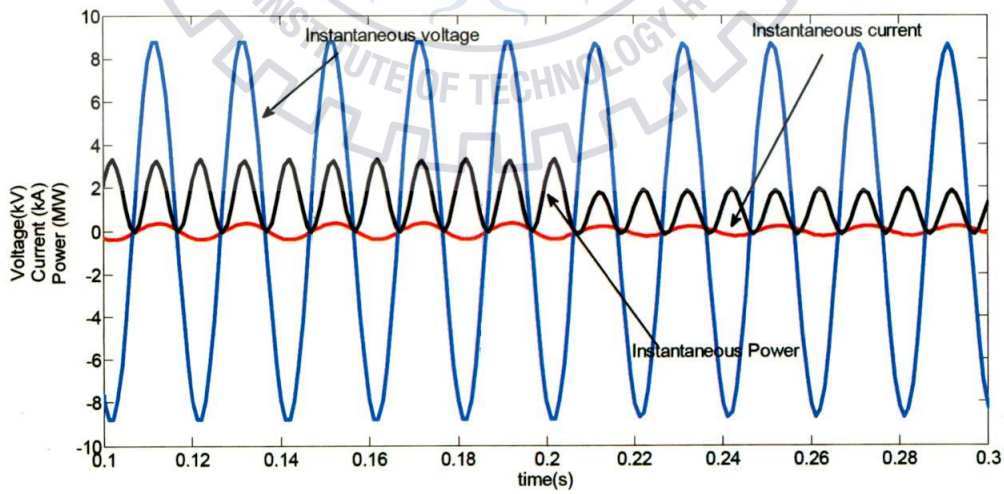

Fig.14. Single phase instantaneous voltage, current and power at DG-1 location during islanding condition for phase 'b'

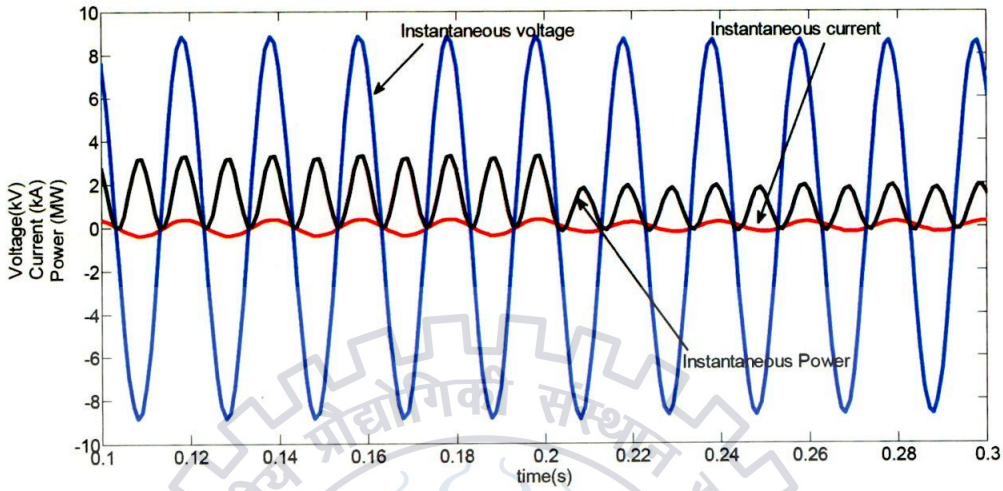

Fig.15. Single phase instantaneous voltage, current and power at DG-1 location during islanding condition for phase 'c'

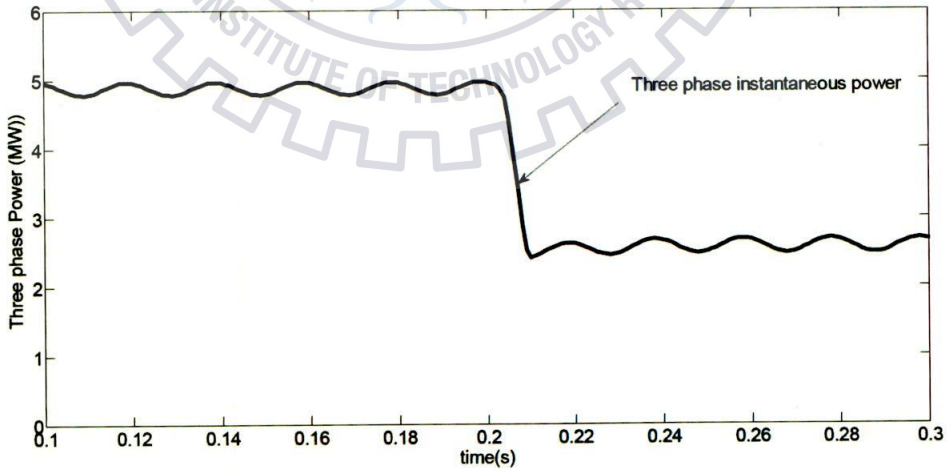

Fig.16. Total three phase instantaneous power at DG-1 location during islanding condition

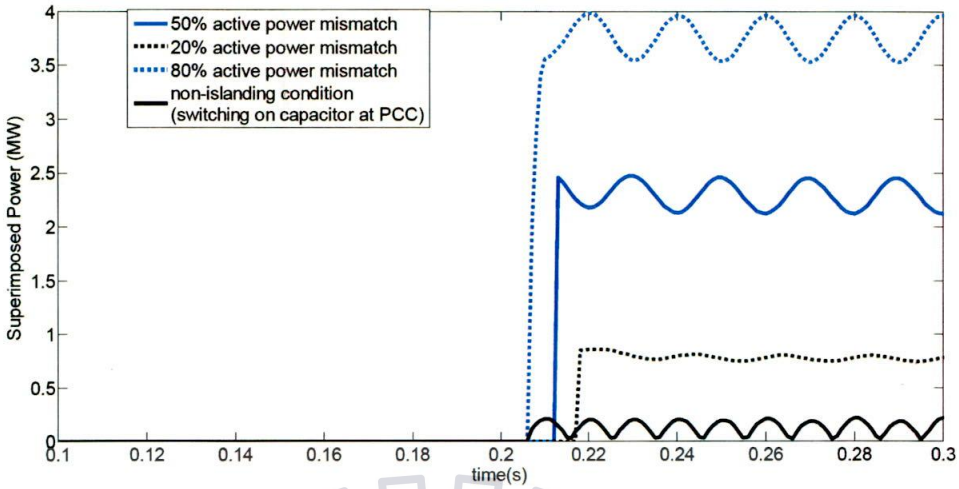

Fig.17. Superimposed power at DG-1 location during islanding at different active power mismatch and a non-islanding condition

After simulating superimposed power for different islanding and non-islanding conditions, cumulative sum of superimposed power is plotted and results have been shown in different figures. Fig.18 shows that simulation results given by the proposed scheme during islanding condition (simulated by the tripping of circuit breakers CB1 and CB2) at 100% active power mismatch with a non islanding condition simulated in the figure by tripping off DG-3. It has been observed that cumulative sum (CUMSUM) during the islanding condition is much higher than non-islanding condition. For CUMSUM threshold has been taken 1.8 pu. Threshold has been decided by simulating all non-islanding conditions and setting to threshold to the greater than the maximum of all these values. Hence the superimposed relay will trip when the measured value of cumulative sum will be higher than threshold value for a certain period of time. In this method this cumulative sum is taken for one period after islanding.

In Fig.19, islanding condition at 80% active power mismatch is shown with a non-islanding condition by switching on the capacitor at the point of common coupling (PCC). Similarly, CUMSUM during islanding condition at 60% active power mismatch and a non-islanding condition by 100% decrease in the local load is simulated in the Fig.20.

Also in the Fig.21 and Fig.22, CUMSUM during islanding condition at 40% and 20% active power mismatch and non-islanding conditions by switching off one 66 kV line Tx-1 and by switching off the transformer1 (Tr-1) are shown respectively.

Fig.23 shows CUMSUM during the islanding condition at different active power mismatch percentages i.e. 5%, 20%, 50% and 80%.

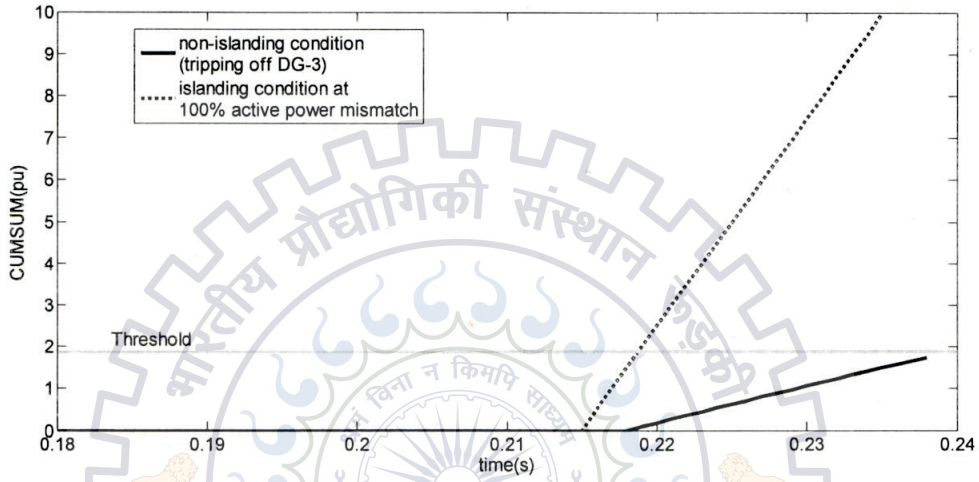

Fig.18. Cumulative sum during islanding at 100% active power mismatch and non-islanding condition

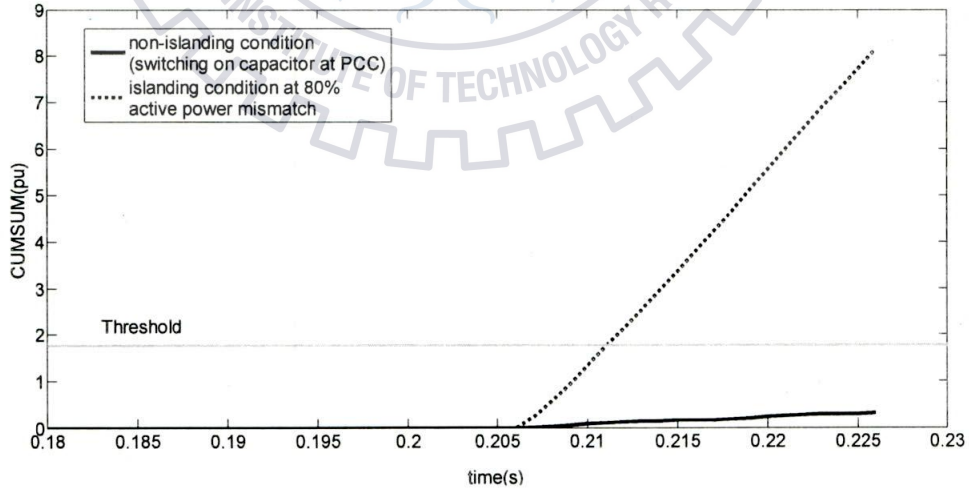

Fig.19. Cumulative sum during islanding at 80% active power mismatch and non-islanding condition

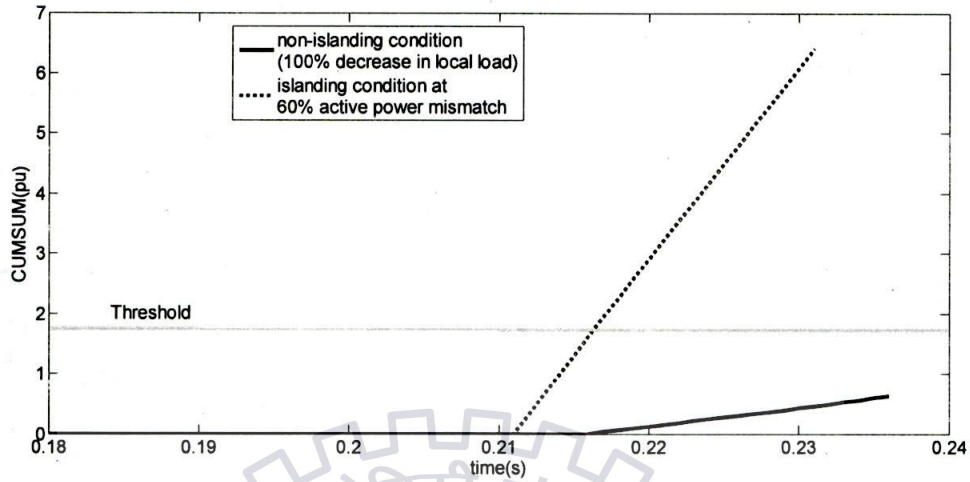

Fig.20. Cumulative sum during islanding at 60% active power mismatch and non-islanding condition

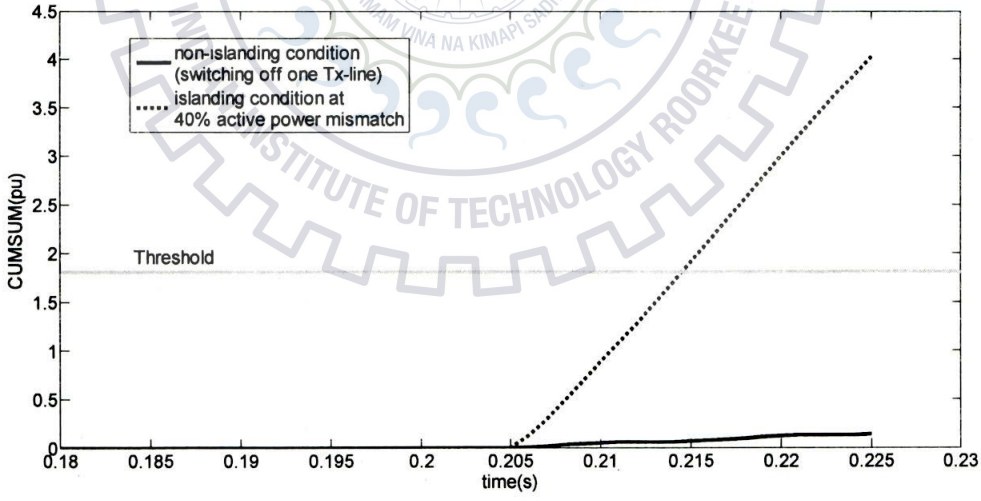

Fig.21. Cumulative sum during islanding at 40% active power mismatch and non-islanding condition

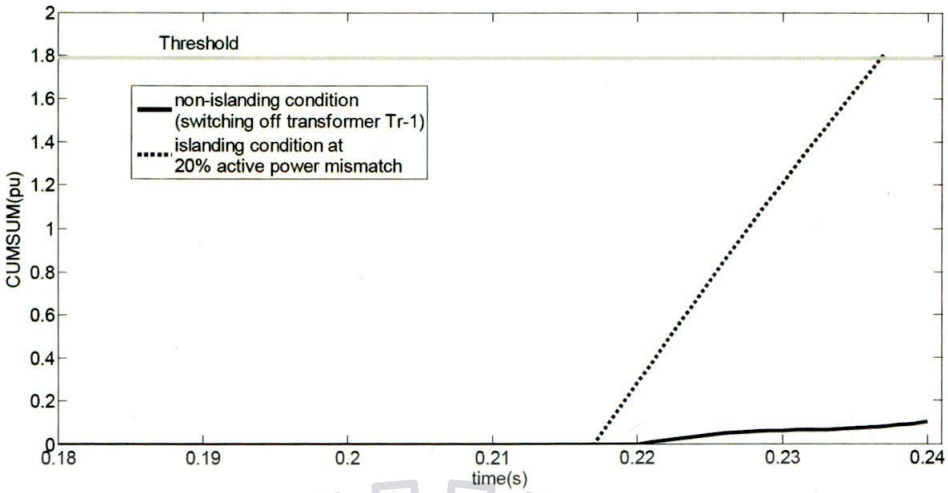

Fig.22. Cumulative sum during islanding at 20% active power mismatch and non-islanding condition

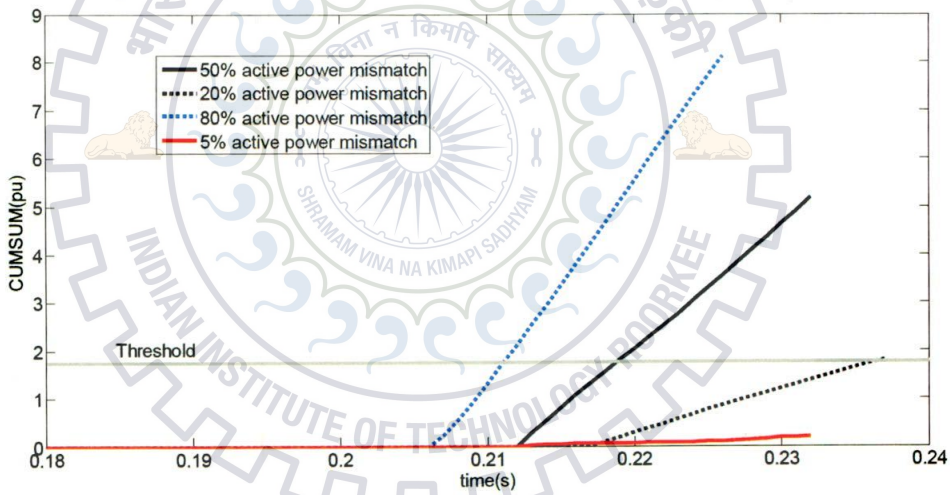

Fig.23. Cumulative sum during islanding at different percentages of active power mismatch

4.3 Comparison of Proposed Technique with Conventional Techniques

In this thesis, comparison of the proposed technique has been done with the two conventional passive techniques i.e. ROCOP and ROCOF. This comparison has been performed by simulating the islanding conditions at various active power mismatches for proposed method as well as for ROCOP and ROCOF. Fig. 24 shows that this comparison of the proposed scheme (CUMSUM) has been done with conventional schemes (ROCOP and ROCOF)

during 20% active power mismatch. All the three methods have been compared with their corresponding threshold values. It is clear by the figure that ROCOP fails to detect the islanding condition for 20% active power mismatch as the ROCOP is below the threshold i.e. 0.16 pu. ROCOF also fails to detect this islanding condition for 20% active power mismatch as the ROCOF is below the threshold i.e. 0.6 Hz/sec. But this figure clearly shows that proposed technique works satisfactorily for 20% active power mismatch as the CUMSUM is above the threshold i.e. 1.8 pu.

Similarly in the Fig. 25, this comparison of the proposed scheme (CUMSUM) has been done with conventional schemes (ROCOP and ROCOF) during 30% active power mismatch. All the three methods have been compared with their corresponding threshold values. It is clear by the figure that ROCOP fails to detect the islanding condition for 30% active power mismatch as the ROCOP is below the threshold i.e. 0.16 pu. ROCOF also fails to detect this islanding condition for 30% active power mismatch as the ROCOF is below the threshold i.e. 0.6 Hz/sec. But this figure clearly shows that proposed technique works satisfactorily for 30% active power mismatch as the CUMSUM is above the threshold i.e. 1.8 pu. Hence proposed scheme successfully operates for active power mismatch above 20%.

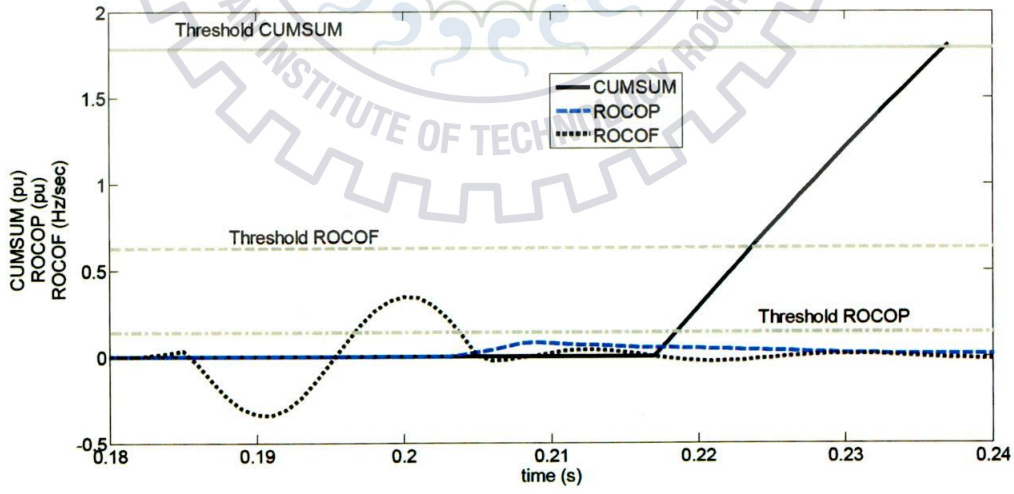

Fig.24. Comparison of the proposed scheme (CUMSUM) with conventional schemes (ROCOP and ROCOF) during 20% active power mismatch

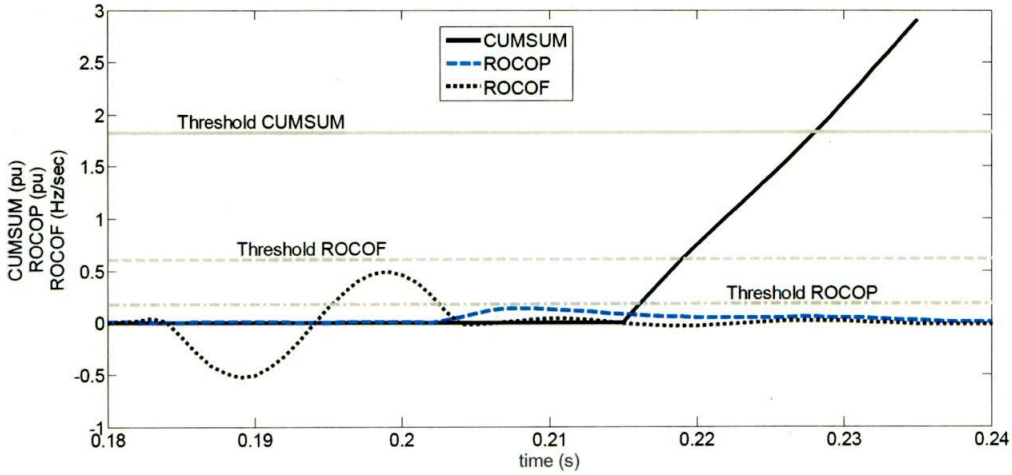

Fig.25. Comparison of the proposed scheme (CUMSUM) with conventional schemes (ROCOP and ROCOF) during 30% active power mismatch

TABLE IV. COMPARISON OF PROPOSED TECHNIQUE WITH ROCOP AND ROCOF

Different percentage of Active power	ROCOP	ROCOF	CUMSUM
0%	×	×	×
5%	×	×	×
10%	×	×	×
20%	×	×	√
30%	×	×	√
40%	√	√	√
50%	√	√	√
60%	√	√	√
80%	√	√	√
90%	√	√	√
100%	√	√	√

√= technique operates in the corresponding condition and detects the islanding condition.

×= technique does not operate in the corresponding condition and unable to detect the islanding condition.

From the Table IV, it is clear that the ROCOP and ROCOF do not operate in the condition if active power mismatch is below 40%. But the proposed technique successfully operates in the condition if active power mismatch is above 20%. Ideally, it is required to disconnect DG from the main power system within 2 sec from the condition of islanding but proposed technique operates within one cycle only i.e. 20 ms. Hence this new technique is very fast in islanding detection as its working depends upon the instantaneous power at DG location.

5 CONCLUSION AND FUTURE SCOPE

In this report, various passive islanding detection techniques based on voltage, frequency, power and impedance are described and a new method based on the cumulative sum of superimposed power is given. Simulation results are also generated to verify the new technique and comparison of the new method with the conventional passive islanding detection methods is also given.

In today's scenario where distributed generations are becoming part of the power system due to their various advantages, it will be very harmful to install them from the protection point of view. Hence it is very essential to accurately detect islanding within a certain period of time so that the reliability and quality of the supply can be improved.

Although the proposed method of islanding detection is very fast, still there is a lack of operating zone. Hence to deal with this more study is needed so that this method will work efficiently in every situation. In this thesis, micogrid has been created by the synchronous generators and loads only. So for future interest microgrid environment can be studied with the use of more types of distributed generation i.e. solar, wind etc.

REFERENCES

[1]. C. A. Cañizares, R. P. Behnke, "Trends in Microgrid Control", *IEEE Transactions On Smart Grid*, vol. 5, no. 4, pp. 1905-1919, 2014.

[2]. P. Mahat, Z. C. and B. Bak-Jensen, "Review of Islanding Detection Methods for Distributed Generation", *3rd International Conference on Electric Utility Deregulation and Restructuring and Power Technologies*, pp. 2743-2748, 2008.

[3]. IEEE, "IEEE Standard for Interconnecting Distributed Resources into Electric Power Systems", IEEE Standard 1547TM, June 2003.

[4]. M. A. Refern, O. Usta, and G. Fielding, "Protection against loss of utility grid supply for a dispersed storage and generation unit," *IEEE Transaction on Power Delivery*, vol. 8, no. 3, pp. 948-954, July 1993.

[5]. M. A. Redfern, J. I. Barren, and O. Usta, "A new microprocessor based islanding protection algorithm for dispersed storage and generation units," *IEEE Trans. Power Delivery*, vol. 10, no. 3, pp. 1249-1254, July 1995.

[6]. J. Warin and W. H. Allen, "Loss of mains protection." *ERA Conference on Circuit Protection for Industrial and Commercial Installations*. London, UK, pp. 4.3.1-12. 1990.

[7]. F. Pai, and S. Huang, "A detection algorithm for islanding-prevention of dispersed consumer-owned storage and generating units," *IEEE Trans. Energy Conversion*, vol. 16, no. 4, pp. 346-351, 2001.

[8]. S. I. Jang, and K. H. Kim, "A new islanding detection algorithm for distributed generations interconnected with utility networks," in *Proc. IEEE International Conference on Developments in Power System Protection*, vol.2, pp. 571-574, April 2004.

[9]. S. I. Jang, and K. H. Kim, "An islanding detection method for distributed generations using voltage unbalance and total harmonic distortion of current," *IEEE Tran. Power Delivery*, vol. 19, no. 2, pp. 745-752, April 2004.

[10]. S. Jang, and K. Kim, "Development of a logical rule-based islanding detection method for distributed resources," in *Proc. IEEE Power Engineering Society Winter Meeting*, vol. 2, pp. 800-806, 2002.

[11]. H. Kabayashi, K. Takigawa, and E. Hashimato, "Method for preventing islanding phenomenon on utility grid with a number of small scale PV systems," *Second IEEE Photovoltaic Specialists Conference*, vol.1, pp. 695-700, 1991.

[12]. M. Bakhshi, R. Noroozian, and G. B. Gharehpetiyan, "Passive anti-islanding scheme based on reactive power in smart grids", 2nd Iranian Conference on Smart Grid, pp. 1-7, May 2012.

[13]. P. O' Kane, and B. Fox, "Loss of mains detection for embedded generation by system impedance monitoring," in *Proc. Sixth International Conference on Developments in Power System Protection*, pp. 95-98, March 1997.

[14]. P. H. Shah, and B. R. Bhalja, "A New Rate of Change of Impedance-based Islanding Detection Scheme in Presence of Distributed Generation", Electric Power Components and Systems, vol. 42, no. 11, pp 1172-1180, 2014.

[15]. P. H. Shah, and B. R. Bhalja, "Anti-Islanding Protection of Distributed Generation using Rate of Change of Impedance", *International Journal of Emerging Electric Power Systems*, vol. 14, no. 5, pp. 433-422, 2013.

[16]. J. Yin, L. Chang, and C. Diduch, "Recent Developments in Islanding Detection for Distributed Power Generation", *Large Engineering systems Conference on Power Engineering*, pp 124-128, July 2004.